Available online at www.sciencedirect.com
SCIENCE DIRECT®
Journal of Chromatography A, 1095 (2005) 102–112
JOURNAL OF CHROMATOGRAPHY A
www.elsevier.com/locate/chroma

Alternative approaches for the estimation of the band broadening parameters in single-detection size exclusion chromatography

Jorge R. Vega [a], Irene Schnöll-Bitai [b,*]

[a] *INTEC (Universidad Nacional del Litoral and CONICET), Güemes 3450, 3000 Santa Fe, Argentina*
[b] *University of Vienna, Inst. f. Physikalische Chemie d. Universität Wien, Waehringer Str. 42, A-1090 Vienna, Austria*

Received 10 March 2005; received in revised form 28 July 2005; accepted 1 August 2005
Available online 22 August 2005

Abstract

New approaches for the determination of the extent of symmetric and asymmetric band broadening (BB) in size exclusion chromatography (SEC) are presented. For this purpose raw data was simulated by starting with either a theoretical Poisson number chain length distribution (NCLD), or a log-normal weight chain length distribution (WCLD). Each distribution was first converted to a BB-free mass chromatogram, as typically obtained from a standard differential refractive index detector. Then, the broadened (or "measured") chromatograms were simulated by convoluting the BB-free chromatograms with a BB function, which was assumed to follow symmetrical (Gauss) as well as unsymmetrical (exponentially modified Gauss) function. A broad range of BB parameters (standard deviation, σ_{BB}, and exponential decay, τ_{BB}) was used for the simulations. The approaches are based on the determination of the points of inflection belonging to the peak of the broadened chromatogram, and closed as well as empirically derived equations connecting the peak width, its variance, and the parameters σ_{BB} and τ_{BB}. The developed methods are applicable for Poisson distributions well above a peak chain length of 100.
© 2005 Elsevier B.V. All rights reserved.

Keywords: Band broadening; Exponentially modified Gauss function; Poisson distribution; Gauss distribution

1. Introduction

Size exclusion chromatography (SEC) is regarded as the most convenient way to measure the molar mass distribution (MMD) of a polymer, although nowadays matrix assisted laser desorption ionization (MALDI) is a possible alternative whenever narrow MMDs (with polydispersities smaller than 1.2) are investigated [1–3]. Direct comparison of both techniques should in principle be possible whenever the shortcomings of each method are properly taken into account. Single-detection SEC (typically, a chromatograph fit with a mass detector) is not an absolute method to measure molar masses, as it is necessary to calibrate the system with narrow standards of the same polymer. Provided that the calibration was carried out correctly there remains the problem that the true distribution is changed during the measurement due to the influence of band broadening (BB). This modification is obvious whenever a monodisperse sample (e.g. the flow rate marker) is injected as the chromatogram will be a continuous distribution rather than a single line.

The BB mainly occurs in the fractionation columns, and as a first approximation, one can neglect the extra spreading introduced by the injector, the detector cells, and the interdetector capillaries [4,5]. The BB strongly distorts the chromatogram shapes when analyzing: (a) narrow chromatograms of half-widths close to those of uniform samples [6–9]; and (b) broad but multimodal chromatograms, with sharp elbows and/or narrow peaks [10–12]. Therefore, it is essential to determine the extent of BB and to apply methods correcting for the detrimental effect of BB.

Correction for BB in SEC has been extensively treated in the literature through different approaches. For the traditional SEC/differential refractometer (DR) configuration, the BB correction aims at obtaining the corrected mass chromatogram by inverting the phenomenological Tung's model [13]. For such

* Corresponding author. Tel.: +43 1 4277 52441; fax: +43 1 4277 9524.
E-mail address: irene.schnoell-bitai@univie.ac.at (I. Schnöll-Bitai).

0021-9673/$ – see front matter © 2005 Elsevier B.V. All rights reserved.
doi:10.1016/j.chroma.2005.08.003

inversion, several approaches have been proposed, which use either analytical [14] or numerical [15] methods. While analytical methods assume a Gaussian BB function, some numerical methods can be implemented for any BB shape. Then, the corrected MMD is obtained by combining the corrected mass chromatogram with an independently determined molar mass calibration. An alternative approach (that does not require inversions) is based on the assumption of a Gaussian BB, and only involves a counterclockwise rotation of the molar mass calibration curve [16,17]. Several BB correction methods have also been proposed for multidetection SEC. Some numerical methods aim at inverting the Tung's model extended to molar mass sensor, while the "true" molar mass calibration may be simultaneously estimated from a corrected chromatograms ratio [7,18]. To directly estimate the MMD, some methods that avoid numerical inversions have also been proposed [6,19]. Correction for BB is beyond the scope of the present article, and will not be further discussed. Most of the procedures have recently been reviewed [8].

There are several approaches to determine the extent of BB. The very first was based on assuming that the total variance of the measured chromatogram (σ^2_{SEC}), can be evaluated from the contributions of the sample variance (σ^2_{PDI}) (based on its polydispersity index, PDI) plus the variance of the BB effect (σ^2_{BB}). Thus,

$$\sigma^2_{SEC} = \sigma^2_{PDI} + \sigma^2_{BB} \quad (1)$$

By assuming a narrow and Gaussian MMD, and a molar mass calibration expressed as $M(V) = D_1 \exp(-D_2 V)$, (D_1, D_2 are constants), then σ^2_{PDI} can be calculated from [20]:

$$\sigma^2_{PDI} = \frac{(PDI - 1)(\alpha + 1)}{D_2^2} \quad (2)$$

with

$$\alpha = \frac{11}{4}(PDI - 1) + \frac{137}{12}(PDI - 1)^2 \quad (3)$$

Eqs. (1)–(3) are still used nowadays [21]. As was shown by Knox and McLennan [20], this approach works for low polydispersity values (e.g. PDI < 1.01), and makes use of the polydispersities as given by the supplier of polymer standards. Unfortunately these polydispersities are in most cases too high as was demonstrated by Vander Heyden et al. [22] as well as Lee et al. [23], and will therefore, lead to an underestimation of σ^2_{BB}.

Several other methods for estimating the BB have been developed. For example, a recycle technique of a commercial standard has been proposed to estimate an arbitrary-shaped BB function in single-detection SEC [24]. By assuming a uniform and Gaussian BB with a linear molar mass calibration, it is possible to use SEC with detection of mass and molar-mass for simultaneously estimating the standard deviation of the BB function and the calibration coefficients [25,26]. For multidetection SEC (in most cases a light scattering in combination with a DR), an iterative procedure for simultaneously estimating the MMD and the standard deviation σ_{BB} of a uniform and Gaussian BB function has been proposed [18,27]. This method was theoretically tested on a narrow Schulz-Zimm MMD, and while the original distribution was well recuperated, the standard deviation differed considerably from its original value. Alternatively, if the shape of the MMD is known (e.g. a Poisson distribution on a linear molar mass axis), then the BB function can be estimated from the difference between the mass chromatogram, and its theoretical prediction in the absence of BB [28].

Lately, preparative thermal gradient interaction chromatography [23,29] was used to fractionate already narrowly distributed polymer samples. It was shown that the obtained fractions had polydispersities smaller than 1.005 [30–32], and these fractions were used to determine the BB function. The peak shapes were not symmetric in all cases and could be best fitted with either exponentially-modified Gaussians (EMG) or exponential-Gaussian hybrid functions which deviates from the simple approach of using a symmetrical (Gaussian) BB function.

An IUPAC project is now dedicated to BB in SEC [33], which is based on a state of the art review (which appeared in 2002) [34] and newer results. The calculation or determination of the true MMD will enable the comparison of SEC results with MALDI-ToF results, although the latter are not as ideal or undisturbed as one would hope for (especially when broader distributions are investigated).

As most papers deal with Gaussian BB functions, it is the aim of this contribution to simulate the influence of an asymmetrical (but uniform) BB, characterized by an EMG (of parameters σ_{BB} and τ_{BB}) on different types of distributions. The special case of $\tau_{BB} = 0.0$ mL corresponding to symmetrical Gaussian broadening is included in the simulations. Three approaches for the determination of the BB function from "measured" chromatograms will be presented, provided that the original weight chain length distribution (WCLD) can be assigned as being a Poisson or a log-normal distribution. In the last case, the corresponding corrected chromatogram can be described by a Gauss distribution (as a function of retention volume), which seems to be a common practice in most publications due to the simpler mathematics involved. The proposed approach for log-normal distributions can be used provided that the standard deviation (or alternatively the peak width) may be inferred from the polymerization conditions. One of the methods presented in the following sections can also be used when multimodale distributions are analyzed which are not ideally baseline separated. The use of multimodale distributions necessitates less experimental measurements as for instance mixtures of standards can be used to determine the extent of BB, thus reducing the total analysis time.

2. Simulation of the SEC fractionation

For a given polymer, the NCLD, $n(i)$, and the WCLD, $w(i)$, respectively, represent the number and the weight fractions of the i-mer ($i = 1, 2, \ldots$). Both $n(i)$ and $w(i)$ are discrete and normalized distributions, that verify:

$$w(i) \propto i n(i) \quad (4.a)$$

$$\sum_{i=1}^{\infty} n(i) = \sum_{i=1}^{\infty} w(i) = 1 \tag{4.b}$$

Similarly, the weight MMD, $w(M)$, is directly obtained by changing the abscissa axis of the WCLD from i to $M_0 i$, where M_0 is the molar mass of the repetitive unit.

To simulate the ideal SEC fractionation (without any influence of BB phenomena), we shall restrict our analysis to a linear homopolymer. The following linear molar mass calibration, $\log M(V)$, is adopted:

$$\log M(V) = \log[M_0 i(V)] = a - bV \tag{5}$$

where V is the retention volume and the constants $\{a, b\}$ represent the intercept and the slope of $\log M(V)$, respectively. Implicitly, it is also assumed that all chains with a given chain length i have the same hydrodynamic volume. In the absence of BB, the unbroadened (or "corrected") chromatogram obtained from a DR, $s^{c}_{DR}(V)$, can be calculated from $w(M)$ and $\log M(V)$, while simultaneously compensating for the nonlinear logarithmic transformation described by Eq. (5). Thus, the ordinates of $s^{c}_{DR}(V)$ are [35]:

$$s^{c}_{DR}(V) = K_{DR} w[M(V)] M(V) \tag{6}$$

where K_{DR} is a constant that also includes the detector gain and the slope of the calibration curve which is constant in this case; and $M(V)$ is calculated from Eq. (5). $s^{c}_{DR}(V)$ can be regarded as a continuous signal that is proportional to the mass of the species i eluting in the infinitesimal range $[V, V + dV]$ as in standard SEC the V axis is evenly-spaced (with ΔV being usually small).

Due to BB, a whole distribution of hydrodynamic volumes (and therefore of molar masses) is instantaneously present in the DR cell. Then, the "measured" mass chromatogram $s_{DR}(V)$ is a broadened version of $s^{c}_{DR}(V)$, that can be evaluated through the Tung's equation [13] as follows:

$$s_{DR}(V) = \int_0^{\infty} g(V, \bar{V}) s^{c}_{DR}(\bar{V}) d\bar{V} \tag{7}$$

where $g(V, \bar{V})$ is the (in general, nonuniform) BB function; and $\bar{V}$ is a dummy integration variable that represents an average elution volume. At each $\bar{V}$, a different $g(V)$ function is defined. For any symmetrical $g(V)$ function, $\bar{V}$ is unambiguously assigned at its maximum. For a skewed $g(V)$ function, however, $\bar{V}$ could be located at the mode, the mean, or any other measure of central tendency, and depending on such location $s_{DR}(V)$ may result shifted to either higher or lower elution volumes with respect to $s^{c}_{DR}(V)$. In any case, $g(V)$ is normalized; i.e. $\int_0^{\infty} g(V)\, dV = 1$. For uniform (or elution volume invariant) BB functions, Eq. (7) reduces to the following simpler expression:

$$s_{DR}(V) = \int_0^{\infty} g(V - \bar{V}) s^{c}_{DR}(\bar{V})\, d\bar{V} = g(V) * s^{c}_{DR}(V) \tag{8}$$

where the symbol '*' stands for the standard "convolution product". Based on Eqs. (6) and (8), the normalized chromatograms, $\tilde{s}^{c}_{DR}(V)$ and $\tilde{s}_{DR}(V)$, are calculated as follows:

$$\tilde{s}^{c}_{DR}(V) = \frac{s^{c}_{DR}(V)}{\int_0^{\infty} s^{c}_{DR}(V)\, dV} = \frac{w(V)M(V)}{\int_0^{\infty} w(V)M(V)\, dV} \tag{9.a}$$

$$\tilde{s}_{DR}(V) = \frac{s_{DR}(V)}{\int_0^{\infty} s_{DR}(V)\, dV} = \int_0^{\infty} g(V - \bar{V}) \tilde{s}^{c}_{DR}(\bar{V})\, d\bar{V} = \frac{\int_0^{\infty} g(V - \bar{V}) w(\bar{V}) M(\bar{V})\, d\bar{V}}{\int_0^{\infty} w(V)M(V)\, dV} \tag{9.b}$$

Notice that the normalized chromatograms are independent of K_{DR}, and $\int_0^{\infty} \tilde{s}^{c}_{DR}(V)\, dV = \int_0^{\infty} \tilde{s}_{DR}(V)\, dV = 1$. In a true experimental case, $\tilde{s}_{DR}(V)$ is calculated from the first equality of Eq. (9.b).

2.1. BB function

Throughout this work, we shall consider a uniform and skewed BB function represented by a first-order EMG [36]. Such EMG is defined as the convolution of a Gaussian and an exponential decay function, as follows:

$$g(V) = N_{\bar{V}_{BB}, \sigma_{BB}}(V) * \frac{\exp(-V/\tau_{BB})}{\tau_{BB}} = \frac{1}{\sqrt{2\pi}\sigma_{BB}} \exp\left(-\frac{(V - \bar{V}_{BB})^2}{2\sigma^2_{BB}}\right) * \frac{\exp(-V/\tau_{BB})}{\tau_{BB}} \tag{10}$$

where $\{\bar{V}_{BB}, \sigma_{BB}\}$ are the mean volume and the standard deviation of the Gaussian $N_{\bar{V}_{BB}, \sigma_{BB}}(V)$; and τ_{BB} is the decay time of the exponential function. Notice that $g(V)$ is normalized, and its mean volume $\bar{V}_g$ is given by:

$$\bar{V}_g = \int_0^{\infty} V g(V) dV = \bar{V}_{BB} + \tau_{BB} \tag{11}$$

To guarantee the same mean volume of $s^{c}_{DR}(V)$ and $s_{DR}(V)$ after the convolution of Eq. (8), a BB function with $\bar{V}_g = 0$ is required, and therefore, $\bar{V}_{BB} = -\tau_{BB}$ must be selected. Thus, Eq. (10) reduces to:

$$g(V) = \frac{1}{\sqrt{2\pi}\sigma_{BB}\tau_{BB}} \exp\left[-\frac{(V + \tau_{BB})^2}{2\sigma^2_{BB}}\right] * \exp\left(-\frac{V}{\tau_{BB}}\right) \tag{12}$$

In the limit case of a symmetrical broadening ($\tau_{BB} \to 0$), the term $\{\exp(-V/\tau_{BB})/\tau_{BB}\}$ in Eq. (12) tends to a Dirac delta and, as expected, $g(V)$ becomes a zero-mean Gaussian:

$$g(V) = \frac{1}{\sqrt{2\pi}\sigma_{BB}} \exp\left[-\frac{V^2}{2\sigma^2_{BB}}\right] \tag{13}$$

2.2. DR chromatogram for a Poisson NCLD

According to the theoretical work of Flory (see for example Ref. [37]), the polymer obtained through an ideal living anionic

polymerization should exhibit a (discrete) Poisson NCLD given by:

$$n_{\mathrm{P}}(i) = \frac{\exp(-\lambda)\lambda^{i-1}}{(i-1)!} \tag{14.a}$$

where λ is the unique parameter of the distribution. From Eqs. (4.a), (4.b) and (14.a) the corresponding discrete WCLD results:

$$w_{\mathrm{P}}(i) = \frac{i}{\lambda+1}\frac{\exp(-\lambda)\lambda^{i-1}}{(i-1)!} \tag{14.b}$$

It is verified that the mean of $n_{\mathrm{P}}(i)$ and $w_{\mathrm{P}}(i)$ are $\lambda+1$ and $\lambda+2$, respectively.

Consider a hypothetical polystyrene sample ($M_0 = 104.15$ g/mol), with a Poisson NCLD of $\lambda = 150$. The NCLD and the WCLD calculated from Eqs. (14.a) and (14.b) are shown in Fig. 1a). The average molar masses are: $M_n = M_0\sum_i i n(i) = 15727$ (g/mol), and $M_w = M_0\sum_i i w(i) = 15830$ (g/mol); and the polydispersity index is: $M_w/M_n = 1.0066$. The BB function was selected as an EMG with $\sigma_{\mathrm{BB}} = 0.20$ mL and $\tau_{\mathrm{BB}} = 0.25$ mL [Eq. (12)]. An arbitrary BB function (at $\bar{V} = 48$ mL) is shown in Fig. 1b). For the molar mass calibration, the following parameters were adopted: $a = 13.0076$ and $b = 0.179941\ \mathrm{mL}^{-1}$ [Eq. (5)]. The normalized chromatograms, $\tilde{s}^{\mathrm{c}}_{\mathrm{DR}}(V)$ and $\tilde{s}_{\mathrm{DR}}(V)$, were simulated according to Eqs. (5), (9.a), (9.b), (12), (14.a) and (14.b), and are represented in Fig. 1b). All numerical simulations were implemented on the basis of a linear V axis, evenly-spaced with volume increments $\Delta V = 0.005$ mL.

The first derivative of $\tilde{s}_{\mathrm{DR}}(V)$, $h(V)$, exhibits a maximum at $V = V_{\mathrm{low}}$, and a minimum at $V = V_{\mathrm{high}}$, as indicated in Fig. 1c), and the elution volumes $\{V_{\mathrm{low}}, V_{\mathrm{high}}\}$ describe also the location of the two points of inflection of $\tilde{s}_{\mathrm{DR}}(V)$. Following the procedure suggested by one of the authors [10,38,39] these points of inflection can also be used to define the peak width. The ordinate values of the first derivative $\{h(V_{\mathrm{low}}), h(V_{\mathrm{high}})\}$, accordingly, correspond to the slope at the points of inflection and contain valuable information concerning the parameters of the BB function, whereas the ratio $r = h(V_{\mathrm{low}})/h(V_{\mathrm{high}})$ gives some information about the asymmetry or skewness of $s_{\mathrm{DR}}(V)$. For instance, it is easily verified that $r = -1$ for a symmetrical chromatogram (e.g. a Gaussian chromatogram); while for a skewed chromatogram with tailing towards higher elution volumes, $r < -1$.

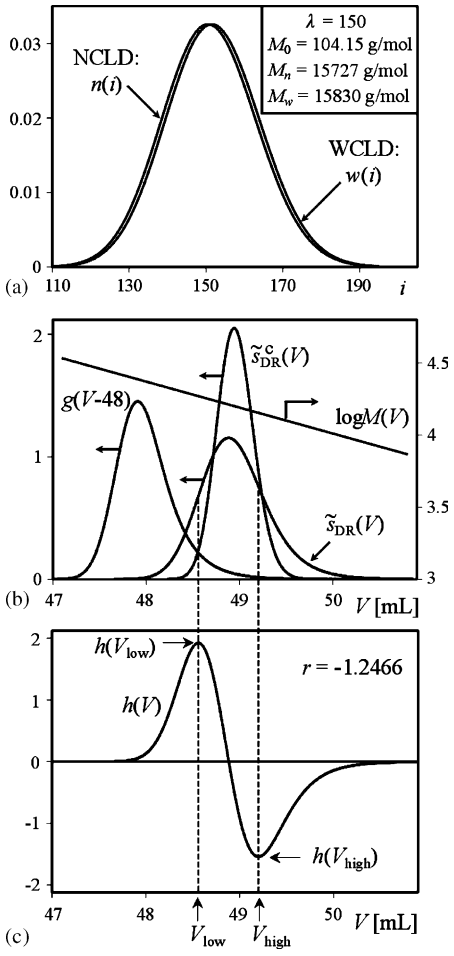

Fig. 1. A theoretical Poisson NCLD with λ = 150 was converted to: (a) a WCLD and (b) an undisturbed $\tilde{s}^{\mathrm{c}}_{\mathrm{DR}}(V)$ through the linear molar mass calibration $\log M(V)$ as well as a broadened chromatographic signal $\tilde{s}_{\mathrm{DR}}(V)$ (with $\sigma_{\mathrm{BB}} = 0.2$ mL and $\tau_{\mathrm{BB}} = 0.25$ mL) (an arbitrary BB function with $\bar{V} = 48$mL is also shown). The first derivative $h(V)$ of the broadened chromatographic signal is shown in (c) together with the coordinates of the points of inflection (V_{low}, V_{high}) and their maximum and minimum in the first derivative.

parameter r. In order to derive a theoretical expression for r the chromatograms obtained from Poisson NCLDs were replaced by corresponding EMG functions of mean volume $\bar{V}_{\mathrm{P}}$ and standard deviation σ_{P} (see Appendix A). It was numerically proven that $\tilde{s}^{\mathrm{c}}_{\mathrm{DR}}(V)$ can be adequately fitted with an EMG function for $\lambda > 100$ [cf. Fig. 6]. Then, the following correlation was derived (see Appendix B):

$$r = \frac{h(V_{\mathrm{low}})}{h(V_{\mathrm{high}})} \cong \frac{(1/\sqrt{2\pi}\sqrt{\sigma^2_{\mathrm{BB}}+\sigma^2_{\mathrm{P}}})\exp(-(V_{\mathrm{low}}-\bar{V}_P+\tau_{\mathrm{BB}})^2/2(\sigma^2_{\mathrm{BB}}+\sigma^2_{\mathrm{P}})) - \tilde{s}_{\mathrm{DR}}(V_{\mathrm{low}})}{(1/\sqrt{2\pi}\sqrt{\sigma^2_{\mathrm{BB}}+\sigma^2_{\mathrm{P}}})\exp(-(V_{\mathrm{high}}-\bar{V}_{\mathrm{P}}+\tau_{\mathrm{BB}})^2/2(\sigma^2_{\mathrm{BB}}+\sigma^2_{\mathrm{P}})) - \tilde{s}_{\mathrm{DR}}(V_{\mathrm{high}})} \tag{15}$$

3. Correlations for the estimation of σ_{BB} and τ_{BB}

3.1. Case 1: Poisson NCLD

According to Eq. (8), both $s^{\mathrm{c}}_{\mathrm{DR}}(V)$ and $g(V)$ contribute to the asymmetry of $s_{\mathrm{DR}}(V)$, and therefore, to the magnitude of the

In Fig. 2, the ratios $r = h(V_{\mathrm{low}})/h(V_{\mathrm{high}})$ obtained from the simulated chromatograms (continuous traces) are compared with their estimation from Eq. (15) (indicated by symbols), for three selected Poisson NCLD (λ = 50, 100, 200), and for several values of σ_{BB} and τ_{BB}, in the ranges: $0.1 \le \sigma_{\mathrm{BB}} \le 0.5$ and $0 \le \tau_{\mathrm{BB}} \le 0.3$. For the two selected limiting values of τ_{BB}, the dashed curves connect the r values calculated from the simulated chromatograms. For low λ, $\tilde{s}^{\mathrm{c}}_{\mathrm{DR}}(V)$ cannot be adequately fitted

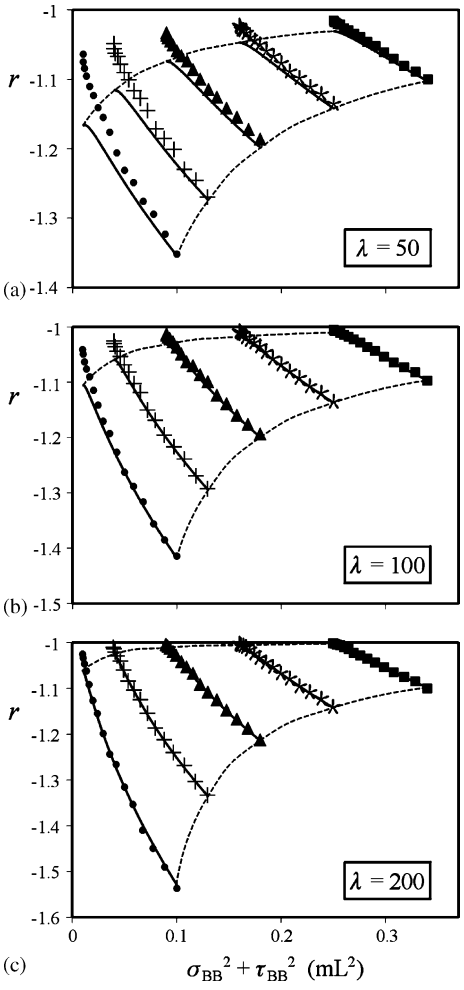

Fig. 2. The ratio $r = h(V_{low})/h(V_{high})$ as a function of the BB variance $\sigma_{BB}^2 + \tau_{BB}^2$ for three Poisson NCLD. The full line connects the results obtained from the simulations, the points were calculated with r.h.s. of Eq. (15) and the corresponding σ_P values (as given in the Appendix A). The upper dashed curve connects the results for τ_{BB} =0.0 mL, whereas $\tau_{BB} = 0.3$ mL for the lower dashed curve. Different σ_{BB} values are represented by the following symbols: (●) 0.1, (×) 0.2, (▲) 0.3, (*) 0.4, (■) 0.5.

with an EMG, and therefore, discrepancies in r are observed at low values of σ_{BB} and τ_{BB} (see Fig. 2a). For $\tau_{BB} \approx 0$, $g(V)$ is a Gaussian function [Eq. (13)], and the asymmetry of $\tilde{s}_{DR}(V)$ ($r < -1$) is exclusively determined by the asymmetry of the NCLD. The symmetry of a Poisson NCLD increases with λ, and therefore, for $\lambda > 200$ and $\tau_{BB} = 0$, $\tilde{s}_{DR}(V)$ is almost symmetric yielding $r \approx -1$. It can be seen for $\lambda = 200$ (Fig. 2c) how r is slightly lower than -1 for small values of σ_{BB} and converges very fast towards -1 for higher σ_{BB} values. In contrast, for low λ values (e.g. $\lambda = 50$), $\tilde{s}_{DR}(V)$ is skewed even for $\tau_{BB} = 0$, and $r < -1$ (see Fig. 2a). On the other hand, r becomes almost independent of λ at high values of σ_{BB} and τ_{BB}.

To estimate both σ_{BB} and τ_{BB} from Eq. (15), it is necessary to develop at least a second independent correlation of these two variables. By analysing the DR chromatograms (simulated for several values of λ, σ_{BB}, and τ_{BB}), two independent correlations were found. The first correlation is as follows:

$$(\Delta[s_{DR}(V)])^2 = (\Delta[s_{DR}^c(V)])^2 + 4\sigma_{BB}^2 + 2\tau_{BB}^2 \quad (16)$$

where $\Delta[s_{DR}(V)] = V_{high} - V_{low}$ is a measure of the experimental peak width defined via the location of the points of inflection; and $\Delta[s_{DR}^c(V)]$ is the theoretical peak width in absence of BB. Whenever multimodale distributions composed of either truly or almost baseline separated Poisson peaks are used this approach can be chosen.

The second correlation is based on the variance of $s_{DR}(V)$, $\mathrm{Var}[s_{DR}(V)]$, which can be determined with accuracy only for truly baseline separated peaks (because of the necessary choice of integration limits):

$$\mathrm{Var}[s_{DR}(V)] = \mathrm{Var}[s_{DR}^c(V)] + \sigma_{BB}^2 + \tau_{BB}^2 \quad (17)$$

in which $\mathrm{Var}[s_{DR}^c(V)]$ is the variance of the unbroadened chromatogram. Both additional correlations of Eqs. (16) and (17), require some knowledge about $s_{DR}^c(V)$ to evaluate either $\Delta[s_{DR}^c(V)]$ or $\mathrm{Var}[s_{DR}^c(V)]$. It was already shown [38–40] that the unbroadened peak width corresponding to a Poisson NCLD can be approximated by:

$$\Delta[s_{DR}^c(V)] \cong \frac{1}{b} \log\left[\frac{\lambda + \sqrt{\lambda}}{\lambda - \sqrt{\lambda}}\right] \quad (18)$$

where λ can be calculated from the PDI of the sample, on the basis of the following relationship:

$$\mathrm{PDI}_{Poisson} \cong 1 + \frac{1}{\lambda} \quad (19)$$

Strictly speaking, λ should be replaced by λ + 1 in Eqs. (18) and (19). However, for typical values of $\lambda > 100$, the experimental accuracy is not high enough to detect the resulting deviations in $\Delta[s_{DR}^c(V)]$ or $\mathrm{PDI}_{Poisson}$ (smaller than 1% in most cases).

On the other hand, $\mathrm{Var}[s_{DR}^c(V)]$ can be estimated in a first approximation through the Knox equation [20] [cf. Eqs. (2), (3), (5) and (19)]:

$$\mathrm{Var}[s_{DR}^c(V)] \cong \frac{1/\lambda + (11/4)/\lambda^2 + (137/12)/\lambda^3}{b^2 \ln^2(10)} \quad (20)$$

By inserting Eq. (18) into Eq. (16), and Eq. (20) into Eq. (17), the following correlations are obtained:

$$\Delta[s_{DR}(V)] \cong \sqrt{\frac{1}{b^2}\log^2\left[\frac{\lambda + \sqrt{\lambda}}{\lambda - \sqrt{\lambda}}\right] + 4\sigma_{BB}^2 + 2\tau_{BB}^2} \quad (21.a)$$

$$\mathrm{Var}[s_{DR}(V)] \cong \frac{1/\lambda + (11/4)/\lambda^2 + (137/12)/\lambda^3}{b^2 \ln^2(10)} + \sigma_{BB}^2 + \tau_{BB}^2 \quad (21.b)$$

For two Poisson NCLD ($\lambda = 50$ and $\lambda = 200$), (Figs. 3 and 4) show the correlations of Eqs. (21.a) and (21.f). Both $\Delta[s_{DR}(V)]$ and $\mathrm{Var}[s_{DR}(V)]$ were directly calculated from the simulated DR chromatograms, and their values are represented by continuous traces; while the r.h.s. terms of Eqs. (21.a) and (21.f) are represented by dots. The r.h.s of Eq. (21.a) acceptably estimates $\Delta[s_{DR}(V)]$; except for high values of τ_{BB}/σ_{BB}, where

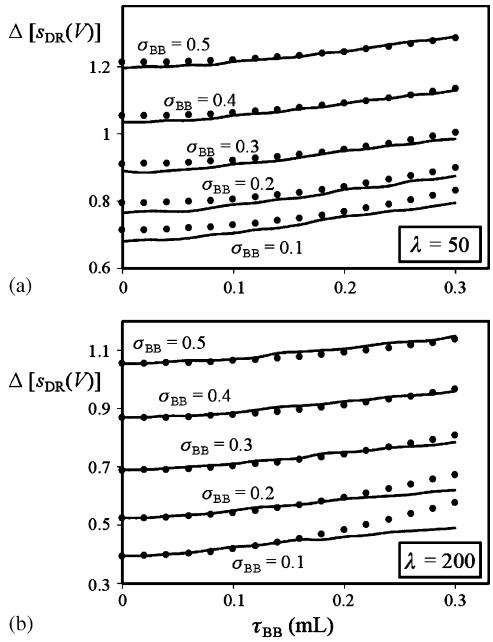

Fig. 3. The peak width of two Poisson distributions defined via the points of inflection [Eq. (16)] as a function of τ_{BB} for several σ_{BB} values (as indicated): full curve connects the results from the simulations, points were calculated with Eq. (21.a).

the highly skewed BB functions strongly distort the shape of the unbroadened chromatogram. The r.h.s. term of Eq. (21.b) accurately estimates Var[$s_{DR}(V)$] for Poisson NCLD of $\lambda > 100$. For $\lambda < 100$, Var[$s_{DR}(V)$] is overestimated because the Knox correlation overrates the variance of the unbroadened chromatogram.

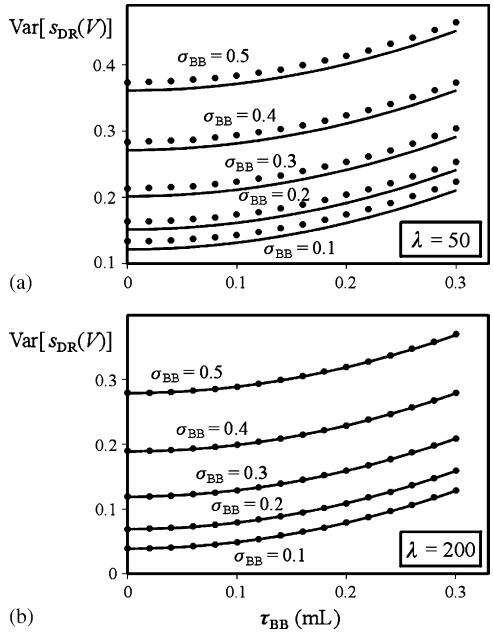

Fig. 4. The variance of two Poisson distributions as a function of τ_{BB} for several σ_{BB} values (as indicated): full curve connects the results from the simulations, points were calculated with Eq. (21.b).

3.2. Case 2: log-normal WCLD

When a log-normal WCLD is combined with a linear molar mass calibration [cf. Eq. (5)], the resulting corrected chromatogram follows a Gaussian function described through:

$$\tilde{s}^{c}_{DR}(V) = \frac{1}{\sqrt{2\pi}\sigma_G} \exp\left(-\frac{(V-\bar{V}_G)^2}{2\sigma_G^2}\right) \tag{22}$$

where $\{\bar{V}_G, \sigma_G\}$ represent the mean volume and the standard deviation of the Gaussian, respectively. In the case of a Gaussian BB, $\tilde{s}_{DR}(V)$ becomes a Gaussian function too (because the convolution of two Gaussian yields a new Gaussian of mean volume $\bar{V}_G$, and variance given by $\sigma_G^2 + \sigma_{BB}^2$. In such case, it can be easily shown that the r value of $\tilde{s}_{DR}(V)$ is always -1, as the slope at the points of inflection depends on the standard deviation and differs only in the algebraic sign. Whenever asymmetric broadening is involved [Eq. (12)] the ratio will become smaller than -1. A similar procedure to that of Appendix B was developed in this case, and the following correlation was obtained:

$$r = \frac{h(V_{low})}{h(V_{high})} = \frac{\varepsilon + \Delta[s_{DR}(V)]}{\varepsilon - \Delta[s_{DR}(V)]} \exp\left(-\frac{\varepsilon\Delta[s_{DR}(V)]}{2(\sigma_G^2 + \sigma_{BB}^2)}\right) \tag{23}$$

with $\varepsilon = 2(\bar{V}_G - \tau_{BB} - V_{low}) - \Delta[s_{DR}(V)]$. Eqs. (16) and (17) remain valid but the corresponding equations for the difference $\Delta\left[s^{c}_{DR}(V)\right]$ and the correct variance must be used instead:

$$\Delta[s^{c}_{DR}(V)] = 2\sigma_G \tag{24.a}$$

$$\mathrm{Var}[s^{c}_{DR}(V)] = \sigma_G^2 \tag{24.b}$$

leading to

$$\Delta[s_{DR}(V)] \cong 2\sqrt{\sigma_G^2 + \sigma_{BB}^2 + \frac{\tau_{BB}^2}{2}} \tag{21.c}$$

$$\mathrm{Var}[s_{DR}(V)] \cong \sigma_G^2 + \sigma_{BB}^2 + \tau_{BB}^2 \tag{21.d}$$

Whenever the BB process is purely symmetric then $\tau_{BB} = 0$ and Eq. (23) yields again $r = -1$ as $\bar{V}_G - V_{low} = \frac{1}{2}\Delta[s_{DR}(V)]$.

4. Strategies to estimate the BB parameters

The decision which combination of equations should be used to determine the BB parameters depends on the available information about the analyzed polymer. Several case scenarios can be thought of and are enumerated and critically reviewed. A general criterion is whether the peaks are truly baseline separated or only approximately baseline separated. In the first case, variances can be determined via the standard procedure of summing the weighted signal heights:

$$\mathrm{Var}[s_{DR}(V)] = \frac{1}{\sum_{j=1}^{n} s_{DR}(V_j)} \times \sum_{i=1}^{n} \left\{ \left(V_i - \frac{\sum_{j=1}^{n} V_j s_{DR}(V_j)}{\sum_{j=1}^{n} s_{DR}(V_j)} \right)^2 s_{DR}(V_i) \right\} \tag{25}$$

In the latter case, the error in the variance will increase with decreasing resolution (i.e. strong overlapping of peaks), due to the distribution cut off by the deliberate choice of summation limits. For slightly overlapping peaks the recommendation is therefore to use the peak width defined via the points of inflection rather than the variance of the distribution.

4.1. Poisson NCLD

From a kinetic point of view, a Poisson NCLD is expected for anionic polymerizations with peak chain lengths ranging from 200 [41] to approximately 10,000. The advantage of such a distribution is that the location of the peak maximum is the essential parameter. Without additional information it is necessary to give an estimate of the maximum error that is introduced whenever λ is determined from the experimentally measured chromatogram. It can be shown (by a procedure similar to the one described in [38]) that the location of the peak maximum of the corresponding WCLD can be approximately described by

$$i_{\max}(\mathrm{WCLD}) \cong \lambda + 1.5 \tag{26.a}$$

$$V_{\max}(\tilde{s}^{c}_{DR}) \cong \frac{a - \log[M_0(i_{\max}+1)]}{b} \tag{26.b}$$

$$V_{\max}(\tilde{s}^{c}_{DR}) \cong \frac{a - \log[M_0(\lambda+2.5)]}{b} \tag{26.c}$$

i.e. $V_{\max}(\tilde{s}^{c}_{DR})$ is shifted to a somewhat lower elution volume with respect to the volume at which a hypothetical uniform sample of chain length λ would elute. From Eq. (26.a) it is obvious that the agreement between $i_{\max}$ and λ becomes better for higher λ values. For a NCLD with λ = 150 the location of the peak maximum in the unbroadened chromatogram $\tilde{s}^{c}_{DR}(V)$ should be at an equivalent chain length (λ + 2.5) of 152.5 which corresponds to 48.942 mL [cf. Fig. 1]. Unfortunately, in practice Eq. (26.c) only can be used by evaluating the maximum of the "experimental" chromatogram, which is further shifted to a lower elution volume due to the influence of the asymmetric broadening. In the case of Fig. 1, the maximum is detected at 48.885 mL which corresponds to an equivalent chain length of approximately 156. This introduces an error in the estimated λ of +2.3% when Eqs. (26.a)–(26.c) are used. Also, the "true" peak width calculated according to Eq. (18) is slightly lower by about 1.4%, and the variance is also underestimated by 1.0% when Eq. (20) is used. Based on several simulations, it was verified that: (a) λ is overestimated, except for extremely low values of τ_{BB}; (b) the estimation error increases with λ for λ < 1000, while it is approximately constant for λ > 1000; and (c) for a given λ, the estimation error increases with τ_{BB} (at a fixed σ_{BB}), and with τ_{BB}/σ_{BB} (at a fixed τ_{BB}). For typical values of σ_{BB} and τ_{BB}, estimation errors lower than 7% are to be expected. For instance, with the BB parameters of Fig. 1, the error would be lower than 4% for any Poisson NCLD.

The calculation of λ with Eq. (19) from a given polydispersity (as given, e.g. by the supplier of polymer standards) is susceptible to the introduction of a considerable error (in some cases leading to an underestimation of λ by more than 50%). Therefore, it is recommended to determine λ from the location of the peak maximum unless the polydispersity is given with an extremely high accuracy. In principle, MALDI measurements can also be used to determine λ and the polydispersity.

Once a given value of λ has been determined, three different combinations of the derived correlations may be selected to estimate σ_{BB} and τ_{BB}: (i) Eqs. (15) and (21.a); (ii) Eqs. (15) and (21.b); and (iii) Eqs. (21.a) and (21.b). In cases (i) and (ii), Eqs. (A.4) and (A.5.a) must also be used to estimate the parameters $\{\bar{V}_P, \sigma_P\}$ required by Eq. (15). In any case, the sign of τ_{BB} must be deduced from the peak shape itself, but it will be positive except for a rather uncommon case of strongly negative skewness of the BB function (i.e. whenever such negative skewness more than compensate the positive skewness of $s^{c}_{DR}(V)$). Except for slightly negative τ_{BB}'s, the r value will indicate the sign of τ_{BB}: for values smaller (greater) than −1 is $\tau_{BB} > 0$ ($\tau_{BB} < 0$). When a multimodal chromatogram is available (where the peaks are not baseline separated), the combination (i) should be chosen. Due to the overestimation of λ, both $\bar{V}_P$ and σ_P are underestimated as can be derived from the simulation results summarized in Fig. 6a); however, the resulting error propagation through Eq. (15) is relatively small.

4.2. Log-normal WCLD

Whenever polymer distributions are discussed in polymer textbooks [42] the log-normal distribution function is included, although in most cases information about the type of polymerization (or polymerization conditions) which should yield such a distribution is missing. In some cases the log-normal distribution is used for an approximate description of, e.g. the distribution of crosslinked photopolymers [43]. If polydispersities are smaller than 1.2 MALDI could give information about the number and mass average degree of polymerization [1–3], and consequently the polydispersities, which can be used to calculate the contribution σ^2_{PDI} [according to Eqs. (2) and (3)], as a way of estimating the peak width and/or the variance of the unbroadened chromatogram [as given by Eqs. (24.a) and (24.b)].

Comparison of the unbroadened and "experimental" chromatogram again shows that the location of the peak maximum $\bar{V}_G$ is shifted to lower values. The extent of the peak shift reduces with large σ_{BB} and small τ_{BB}. The simulations also showed that Eq. (16) remains valid, whereas the correctness of Eq. (17) is usually agreed upon. Eqs. (24.a) and (24.b) together with Eqs. (16) and (17) can be used whenever σ_G is known with sufficient accuracy.

In Fig. 5, the excellent agreement between the r values determined from the simulated distributions (full curves) and those calculated with Eq. (23) (dots) can be seen. The broader the original distribution the less pronounced is the influence of the BB parameters on r. A high accuracy of the input values $\bar{V}_G$ and σ_G is essential for reasonable results. In principle, again three different combinations of correlations can be chosen to estimate σ_{BB} and τ_{BB}: (i) Eqs. (23) and (21.c); (ii) Eqs. (23) and (21.d); and (iii) Eqs. (21.c) and (21.d). For the first two cases τ_{BB} can be calculated from the rearranged Eqs. (21.c) and (21.d),

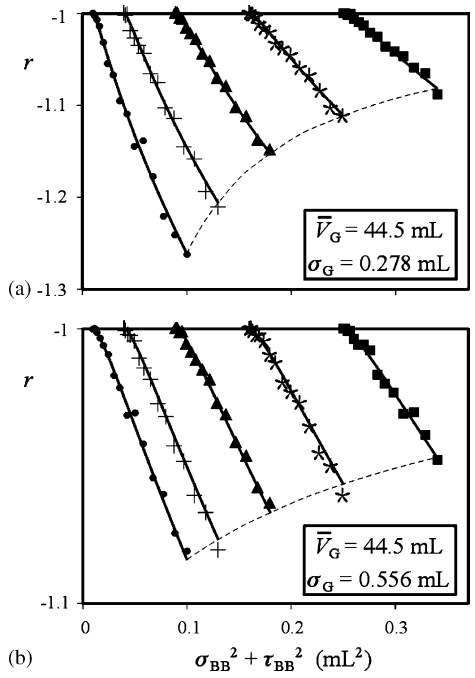

Fig. 5. The ratio $r = h(V_{low})/h(V_{high})$ as a function of the total variance $\sigma_{BB}^2 + \tau_{BB}^2$ for two log-normal WCLD of different variances. The full line connects the results obtained from the simulations, the points were calculated with r.h.s. of Eq. (23). The dashed curve connects the results for $\tau_{BB} = 0.3$ mL.

respectively

$$\tau_{BB} \cong \sqrt{\frac{1}{2}\Delta[s_{DR}(V)]^2 - 2(\sigma_G^2 + \sigma_{BB}^2)} \quad (21.c)$$

$$\tau_{BB} \cong \sqrt{\mathrm{Var}[s_{DR}(V)] - (\sigma_G^2 + \sigma_{BB}^2)} \quad (21.d)$$

which are to be inserted into Eq. (23), thus reducing the problem to solve Eq. (23) in order to obtain $\sigma_G^2 + \sigma_{BB}^2$ and consequently σ_{BB}. For the last case (iii), Eqs. (21.c) and (21.d) yield:

$$\sigma_{BB} \cong \sqrt{\frac{1}{2}\Delta[s_{DR}(V)]^2 - \mathrm{Var}[s_{DR}(V)] - \sigma_G^2} \quad (21.e)$$

$$\tau_{BB} \cong \sqrt{2\mathrm{Var}[s_{DR}(V)] - \frac{1}{2}\Delta[s_{DR}(V)]^2} \quad (21.f)$$

5. Conclusions

A method capable to determine BB parameters including both cases of (symmetric) Gaussian and (asymmetric) EMG functions was developed based on simulated distribution curves. It is important to be able to discern the actual BB function as the peak shape is a fundamental parameter [44] which is influenced by the experimental parameters and gives access to an improved understanding of the separation mechanism.

The advantage of the presented methods is that no numerical inversion procedure is necessary. The general procedure requires the numerical differentiation of the experimental signal together with the determination of the maximum location, the variance, and/or the points of inflection. The newly defined ratio of the slopes at the points of inflection (which are simply the ordinate values at the maximum and minimum in the first derivative) gives immediate information about the existence of asymmetry in the peak shape. The experimental ratio is equal to −1 only for symmetric peaks; it will be smaller than −1 as soon as any kind of asymmetry occurs for $\tau_{BB} > 0$ (a case already observed by Busnel et al. [29]). From a mathematical point of view ratios greater than −1 are to be expected for $\tau_{BB} < 0$, although no such case was observed experimentally to the best of our knowledge till now. Whenever either the true (or correct) distribution or the function describing the BB process or both deviate from a simple Gauss distribution the experimentally measured peaks will be skewed and the r value will deviate from −1.

Another test to find out whether symmetric or asymmetric broadening takes place can be done with the aid of Eqs. (21.a)–(21.f), however, the knowledge of some information concerning the true distribution (Poisson or log-normal) is necessary in this case. In all, the simple structure of the developed equations are favourable for a transparent determination of the BB parameters.

Finally, the applicability of the presented equations is not restricted to the direct determination of BB parameters but can also be used either as an independent consistency check of BB parameters derived, e.g. by inversion procedures or as a good estimate to start the inversion procedures with.

Acknowledgements

This work was carried out in the frame of Project 2003-023-2-G.Meira (IUPAC): “Data Treatment in the Size Exclusion Chromatography of Polymers” [33]. First author is grateful for the financial support received from the following Argentine institutions: CONICET, Universidad Nacional del Litoral, and SECyT. Fruitful discussions on BB in SEC with Dr. G. Meira are also gratefully acknowledged.

Appendix A. Adjustment of the DR chromatogram of a Poisson NCLD with an EMG

This appendix aims at fitting the normalized corrected DR chromatogram, $\tilde{s}_{DR}^{c}(V)$, corresponding to a homopolymer with a Poisson NCLD of parameter λ [Eq. (14.a) and (14.b)], by means of an EMG function, $\hat{\tilde{s}}_{DR}^{c}(V)$, of parameters $\{\bar{V}_P, \sigma_P, \tau_P\}$. For a linear molar mass calibration $\tilde{s}_{DR}^{c}(V)$ can be simulated through Eqs. (5), (9.a) and (14.b); while $\hat{\tilde{s}}_{DR}^{c}(V)$ is simulated from:

$$\hat{\tilde{s}}_{DR}^{c}(V) = \frac{1}{\sqrt{2\pi}\sigma_P\tau_P} \exp\left(-\frac{(V-\bar{V}_P)^2}{2\sigma_P^2}\right) * \exp\left(-\frac{V}{\tau_P}\right) \quad (A.1)$$

Assume a discrete elution volume axis evenly-spaced (with ΔV) in the range $[V_1 - V_2]$, such as the ordinates of $\tilde{s}_{DR}^{c}(V)$ and $\hat{\tilde{s}}_{DR}^{c}(V)$ outside $[V_1 - V_2]$ can be neglected. A discrete version of V is represented by the vector $\mathbf{V} = [V_1, V_1 + \Delta V, V_1 + 2\Delta V, \ldots, V_2]^T$. (Superscript ‘T’ stands for the transpose vector.) At each component of $\mathbf{V}$, the (column) vectors $\tilde{\mathbf{s}}_{\mathbf{DR}}^{\mathbf{c}}$ and $\hat{\tilde{\mathbf{s}}}_{\mathbf{DR}}^{\mathbf{c}}$ contain the ordinates of $\tilde{s}_{DR}^{c}(V)$ and $\hat{\tilde{s}}_{DR}^{c}(V)$, respectively. The following

extended error vector, **e**, was defined:

$$\mathbf{e} = \begin{bmatrix} \tilde{\mathbf{s}}^{\mathbf{c}}_{\mathbf{DR}} - \hat{\tilde{\mathbf{s}}}^{\mathbf{c}}_{\mathbf{DR}} \\ \Delta V \mathbf{V}^{\mathrm{T}}(\tilde{\mathbf{s}}^{\mathbf{c}}_{\mathbf{DR}} - \hat{\tilde{\mathbf{s}}}^{\mathbf{c}}_{\mathbf{DR}}) \\ \mathrm{Var}[\tilde{s}^{\mathrm{c}}_{\mathrm{DR}}(V)] - \mathrm{Var}[\hat{\tilde{s}}^{\mathrm{c}}_{\mathrm{DR}}(V)] \end{bmatrix} \tag{A.2}$$

The first component of Eq. (A.2), $\tilde{\mathbf{s}}^{\mathbf{c}}_{\mathbf{DR}} - \hat{\tilde{\mathbf{s}}}^{\mathbf{c}}_{\mathbf{DR}}$, is a (column) vector that represents the estimation error in $\tilde{s}^{\mathrm{c}}_{\mathrm{DR}}(V)$ at each discrete volume; while the second and third components are scalar quantities that represent the estimation errors in the mean volume and in the variance of $\tilde{s}^{\mathrm{c}}_{\mathrm{DR}}(V)$, respectively. Then, the values of $\{\bar{V}_{\mathrm{P}}, \sigma_{\mathrm{P}}, \tau_{\mathrm{P}}\}$ can be obtained by solving the following nonlinear least-square problem:

$$J(\lambda) = \min_{\{\bar{V}_{\mathrm{P}}, \sigma_{\mathrm{P}}, \tau_{\mathrm{P}}\}} (\mathbf{e}^{\mathrm{T}}\mathbf{e}) \tag{A.3}$$

where J represents a figure of merit of the mean square estimation error. In Eq. (A.3), the functionality of J with λ has explicitly been included to remind that a different value of J is obtained for each Poisson NCLD of parameter λ.

For $50 \le \lambda \le 400$, and $\log M(V) = a - bV$ ($a = 13.0076$, $b = 0.179941$), the main simulation results are shown in Fig. 6. The parameters of the adjusted EMGs and J are indicated in Fig. 6a). Since J decreases monotonically with λ, better adjustments of $\tilde{s}^{\mathrm{c}}_{\mathrm{DR}}(V)$ by an EMG are obtained at high values of λ. Fig. 6b shows the agreement between the original (full curve) and the adjusted (dashed curve) chromatograms for two selected distributions of $\lambda = 50$ and $\lambda = 150$. For $\lambda < 50$, $\tilde{s}^{\mathrm{c}}_{\mathrm{DR}}(V)$ cannot acceptably be adjusted by an EMG function.

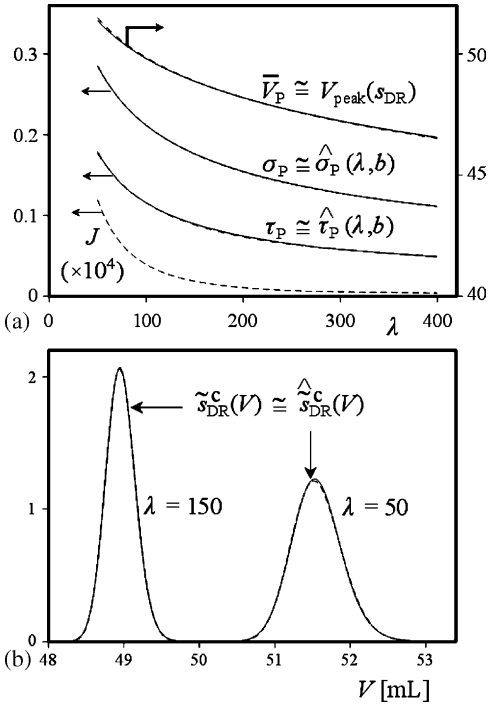

Fig. 6. (a) The parameters $\bar{V}_{\mathrm{P}}$, σ_{P}, τ_{P}, and J (representative for the mean square estimation error) as a function of λ. (b) Full curves: the Poisson WCLDs converted to the chromatographic signals, dashed curves: EMG function calculated with the corresponding parameter triple $\bar{V}_{\mathrm{P}}$, σ_{P}, τ_{P}.

For a broad range of the BB parameters, numerical simulations of the DR chromatograms showed that $\bar{V}_{\mathrm{P}}$ practically coincides with the peak volume of the measured chromatogram, $V_{\mathrm{peak}}(s_{\mathrm{DR}})$. Thus, $\bar{V}_{\mathrm{P}}$ can be estimated as:

$$\bar{V}_{\mathrm{P}} \cong V_{\mathrm{peak}}(s_{\mathrm{DR}}) \tag{A.4}$$

For instance, for $\sigma_{\mathrm{BB}} = 0.20$ mL and $\tau_{\mathrm{BB}} = 0.25$ mL, Fig. 6a) shows $V_{\mathrm{peak}}(s_{\mathrm{DR}})$ (dashed line) practically over-imposed with $\bar{V}_{\mathrm{P}}$.

Even for the common case of PS, the values of σ_{P} and τ_{P} depend on the molar mass calibration parameters (a and b) of the available SEC equipment; and therefore, the proposed method should be implemented for each particular calibration, accordingly. In order to avoid such implementation, the following approximate algebraic correlations for estimating the σ_{P} and τ_{P} have been derived (for PS):

$$\hat{\sigma}_{\mathrm{P}}(\lambda, b) \cong \frac{\sqrt{-(1.256/\lambda^2) + (0.155/\lambda) + 2.38 \times 10^{-5}}}{b} \tag{A.5.a}$$

$$\hat{\tau}_{\mathrm{P}}(\lambda, b) \cong \frac{-(27.70/\lambda^2) + (1.933/\lambda) + 4.342 \times 10^{-3}}{b} \tag{A.5.b}$$

The correlations of Eqs. (A.5.a) and (A.5.b) are shown in Fig. 6a (dashed lines) again for $b = 0.179941$ mL, and practically coincide with the values of σ_{P} and τ_{P} obtained through the optimisation procedure. Only the slope of the calibration curve and λ influence the parameters σ_{P} and τ_{P}.

Appendix B. Derivation of ratio *r* [Eq. (15)]

Consider a homopolymer with a Poisson NCLD of parameter λ [Eq. (14.a)], and its normalized correct chromatogram $\tilde{s}^{\mathrm{c}}_{\mathrm{DR}}(V)$ adjusted by means of an EMG function, $\hat{\tilde{s}}^{\mathrm{c}}_{\mathrm{DR}}(V)$, of parameters $\{\bar{V}_{\mathrm{P}}, \sigma_{\mathrm{P}}, \tau_{\mathrm{P}}\}$ [cf. Appendix A Eq. (A.1)]. The uniform BB function, $g(V)$, is represented by the zero-mean EMG of Eq. (10). Then, $\tilde{s}_{\mathrm{DR}}(V)$ can be calculated from Eqs. (9.a), (9.b), (10) and (11) as follows:

$$\begin{aligned} \tilde{s}_{\mathrm{DR}}(V) &= g(V) * \tilde{s}^{\mathrm{c}}_{\mathrm{DR}}(V) \\ &= \left[N_{-\tau_{\mathrm{BB}}, \sigma_{\mathrm{BB}}}(V) * \frac{\exp(-V/\tau_{\mathrm{BB}})}{\tau_{\mathrm{BB}}} \right] \\ &\quad * \left[N_{\bar{V}_{\mathrm{P}}, \sigma_{\mathrm{P}}}(V) * \frac{\exp(-V/\tau_{\mathrm{P}})}{\tau_{\mathrm{P}}} \right] \end{aligned} \tag{B.1}$$

Bearing in mind that: (i) for two signals y_1 and y_2, $y_1 * y_2 = y_2 * y_1$; and (ii) the convolution of two Gaussian is a new Gaussian: $N_{\bar{V}_1, \sigma_1}(V) * N_{\bar{V}_2, \sigma_2}(V) = N_{\bar{V}_1 + \bar{V}_2, \sqrt{\sigma_1^2 + \sigma_2^2}}(V)$,

then:

$$\tilde{s}_{DR}(V) = N_{-\tau_{BB},\sigma_{BB}}(V) * N_{\bar{V}_P,\sigma_P}(V) * \frac{\exp(-V/\tau_{BB})}{\tau_{BB}} * \frac{\exp(-V/\tau_P)}{\tau_P}$$
$$= N_{\bar{V}_P-\tau_{BB},\sqrt{\sigma_{BB}^2+\sigma_P^2}}(V) * \left[\frac{\tau_P}{\tau_P-\tau_{BB}}\frac{\exp(-V/\tau_P)}{\tau_P} + \frac{\tau_{BB}}{\tau_{BB}-\tau_P}\frac{\exp(-V/\tau_{BB})}{\tau_{BB}}\right] \quad (B.2)$$

In practice $\tau_P \neq \tau_{BB}$, and therefore, Eq. (B.2) can unambiguously be evaluated. Let us define the following auxiliary parameters:

$$\bar{V} = \bar{V}_P - \tau_{BB} \quad (B.3.a)$$

$$\sigma = \sqrt{\sigma_{BB}^2 + \sigma_P^2} \quad (B.3.b)$$

By replacing Eqs. (B.3.a) and (B.3.b) into Eq. (B.2), it results:

$$\tilde{s}_{DR}(V) = \frac{\tau_P}{\tau_P-\tau_{BB}} y_P(V) + \frac{\tau_{BB}}{\tau_{BB}-\tau_P} y_{BB}(V) \quad (B.4)$$

where

$$y_P(V) = N_{\bar{V},\sigma}(V) * \frac{\exp(-V/\tau_P)}{\tau_P} \quad (B.5.a)$$

$$y_{BB}(V) = N_{\bar{V},\sigma}(V) * \frac{\exp(-V/\tau_{BB})}{\tau_{BB}} \quad (B.5.b)$$

Thus, $\tilde{s}_{DR}(V)$ is the weighted sum of two EMGs [$y_P(V)$ and $y_{BB}(V)$], which only differ in the exponential decay term.

Any arbitrary EMG function, $y_0(V)$, of parameters $\{\bar{V}_0, \sigma_0, \tau_0\}$ verifies the following ordinary differential equation:

$$\frac{dy_0(V)}{dV} + \frac{1}{\tau_0} y_0(V) = \frac{1}{\sqrt{2\pi}\sigma_0\tau_0} \exp\left(-\frac{(V-\bar{V}_0)^2}{2\sigma_0^2}\right) = \frac{N_{\bar{V}_0,\sigma_0}(V)}{\tau_0} \quad (B.6)$$

Then, from Eqs. (B.4)–(B.6), the first and second derivatives of $\tilde{s}_{DR}(V)$ are:

$$\frac{d\tilde{s}_{DR}(V)}{dV} = \frac{y_{BB}(V)-y_P(V)}{\tau_P-\tau_{BB}} = \frac{1}{\tau_P}\left[y_{BB}(V) - \tilde{s}_{DR}(V)\right]$$
$$= \frac{1}{\tau_{BB}}[y_P(V) - \tilde{s}_{DR}(V)] \quad (B.7.a)$$

$$\frac{d^2\tilde{s}_{DR}(V)}{dV^2} = \frac{1}{\tau_P-\tau_{BB}}\left[\frac{N_{\bar{V},\sigma}(V)-y_{BB}(V)}{\tau_{BB}} - \frac{N_{\bar{V},\sigma}(V)-y_P(V)}{\tau_P}\right] \quad (B.7.b)$$

At the inflection points (IP), $d^2\tilde{s}_{DR}(V)/dV^2 = 0$. Then,

$$\tau_{BB}\left[y_P(V_{IP}) - N_{\bar{V},\sigma}(V_{IP})\right] = \tau_P[y_{BB}(V_{IP}) - N_{\bar{V},\sigma}(V_{IP})] \quad (B.8)$$

From Eqs. (B.4), (B.7.a), (B.7.b) and (B.8), it is obtained:

$$h(V_{IP}) = \left.\frac{d\tilde{s}_{DR}(V)}{dV}\right|_{V=V_{IP}} = \frac{N_{\bar{V},\sigma}(V_{IP}) - y_P(V_{IP})}{\tau_P} = \frac{N_{\bar{V},\sigma}(V_{IP}) - y_{BB}(V_{IP})}{\tau_{BB}} \quad (B.9)$$

The DR chromatogram has two IP placed at the elution volumes: $\{V_{low}, V_{high}\}$. From Eqs. (B.3.a), (B.3.b), (B.7.a) and (B.9), it results:

$$r = \frac{h(V_{low})}{h(V_{high})} = \frac{(1/\sqrt{2\pi}\sqrt{\sigma_{BB}^2+\sigma_P^2})\exp(-(V_{low}-\bar{V}_P+\tau_{BB})^2/2(\sigma_{BB}^2+\sigma_P^2)) - \tilde{s}_{DR}(V_{low})}{(1/\sqrt{2\pi}\sqrt{\sigma_{BB}^2+\sigma_P^2})\exp(-(V_{high}-\bar{V}_P+\tau_{BB})^2/2(\sigma_{BB}^2+\sigma_P^2)) - \tilde{s}_{DR}(V_{high})} \quad (B.10)$$

References

[1] H. Pasch, W. Schrepp, MALDI-ToF Mass Spectrometry of Synthetic Polymers, Springer-Verlag, Berlin Heidelberg, 2003, p. 112.
[2] S.D. Hanton, Chem. Rev. 101 (2001) 527.
[3] M.W.F. Nielen, Mass Spectrom. Rev. 18 (5) (1999) 309.
[4] A. Prüß, C. Kempter, J. Gysler, T. Jira, J. Chromatogr. A 1016 (2003) 129.
[5] I. Schnöll-Bitai, J. Chromatogr. A 1084 (2005) 160.
[6] P.I. Prougenes, D. Berek, G.R. Meira, Polymer 40 (1998) 117.
[7] J.R. Vega, G.R. Meira, J. Liq. Chrom. Relat. Technol. 24 (7) (2001) 901.
[8] G.R. Meira, J.R. Vega, in: J. Cazes (Ed.), Dekker Encyclopedia of Chromatography, Marcel-Dekker Ed., New York, 2001, p. 71.
[9] I. Schnöll-Bitai, Macromol. Theory Simul. 12 (2003) 111.
[10] I. Schnöll-Bitai, C. Pfeisinger, Macromol. Chem. Phys. 204 (2003) 384.
[11] A. Kornherr, O.F. Olaj, I. Schnöll-Bitai, G. Zifferer, Macromol. Theory Simul. 12 (2003) 259.
[12] A. Kornherr, O.F. Olaj, I. Schnöll-Bitai, G. Zifferer, Macromol. Theory Simul. 13 (2004) 560.
[13] L.H. Tung, J. Appl. Polym. Sci. 10 (1966) 1271.
[14] A.E. Hamielec, in: J. Janca (Ed.), Steric Exclusion Liquid Chromatography of Polymers, Chromatogr. Sci. Ser. 25, M. Dekker Inc., New York, 1984, p. 117.
[15] L.M. Gugliotta, J.R. Vega, G.R. Meira, J. Liq. Chromatogr. 13 (1990) 1671.
[16] W. Yau, H. Stoklosa, D. Bly, J. Appl. Polym. Sci. 21 (1977) 1911.
[17] C. Jackson, W. Yau, J. Chromatogr. 645 (1993) 209.
[18] M. Netopilík, Polym. Bull. 7 (1982) 575.
[19] C. Jackson, Polymer 40 (1999) 3735.
[20] J.H. Knox, F. McLennan, Chromatographia 10 (1977) 75.
[21] S.-T. Popovici, W.Th. Kok, P.J. Schoenmakers, J. Chromatogr. A 1060 (2004) 237.
[22] Y. Vander Heyden, S.-T. Popovici, B.B.P. Staal, P.J. Schoenmakers, J. Chromatogr. A 986 (2003) 1.
[23] W. Lee, H. Lee, J. Cha, T. Chang, K.J. Hanley, T.P. Lodge, Macromolecules 33 (2000) 5115.

[24] D. Alba, G.R. Meira, J. Liq. Chromatogr. 9 (6) (1986) 1141.
[25] K. Lederer, G. Imrich-Schwarz, M. Dunky, J. Appl. Polym. Sci. 32 (1986) 4751.
[26] J. Billiani, G. Rois, K. Lederer, Chromatographia 26 (1988) 372.
[27] M. Netopilik, in: A.M. Striegel (Ed.), ACS Symposium Series 893, American Chemical Society, Washington, DC, pp. 302–318.
[28] I. Schnöll-Bitai, Chromatographia 58 (2003) 375.
[29] J.P. Busnel, F. Foucault, L. Denis, W. Lee, T. Chang, J. Chromatogr. A 930 (2001) 61.
[30] H.C. Lee, T. Chang, S. Harville, J.W. Mays, Macromolecules 31 (1998) 690.
[31] H.C. Lee, W. Lee, T. Chang, J.S. Yoon, D.J. Frater, J.W. Mays, Macromolecules 31 (1998) 4114.
[32] T. Chang, H.C. Lee, W. Lee, S. Park, P. Ko, Macromol. Chem. Phys. 200 (1999) 2188.
[33] G.R. Meira, Data treatment in size exclusion chromatography of polymers—correction for band broadening and other systematic errors. IUPAC Macromolecular División (IV), TGM2003-023-2-400 (2003).
[34] J.L. Baumgarten, J.P. Busnel, G.R. Meira, J. Liq. Chromatogr. Relat. Technol. 25 (13–15) (2002) 1967.
[35] D.W. Shortt, J. Liq. Chromatogr. 16 (16) (1993) 3371.
[36] E. Grushka, Anal. Chem. 44 (11) (1972) 1733.
[37] M. Morton, Anionic Polymerization: Principles and Practice, Academic Press Inc., New York, 1983 (Chapter 8).
[38] I. Schnöll-Bitai, Macromol. Chem. Phys. 203 (2002) 1754.
[39] I. Schnöll-Bitai, Macromol. Theory Simul. 11 (2002) 770.
[40] I. Schnöll-Bitai, Macromol. Theory Simul. 11 (2002) 199.
[41] W. Lee, H. Lee, J. Cha, T. Chang, K.J. Hanley, T.P. Lodge, Macromolecules 33 (2000) 5111.
[42] H.-G. Elias, Markomoleküle—Chemische Struktur und Synthesen, Wiley-VCH, Weinheim, 1999, p. 71.
[43] A. Reiser, Photoreactive Polymers—The Science and Technology of Resists, John Wiley & Sons, New York, 1989, p. 51.
[44] E. Grushka, J. Phys. Chem. 76 (18) (1972) 2586.